ISTITUTO NAZIONALE DI FISICA NUCLEARE
Laboratori Nazionali di Frascati

LNF-77/45(R)
26 Agosto 1977

G. P. Capitani, E. De Sanctis, C. Guaraldo, G. Ricco, M. Sanzone, R. Scrimaglio and A. Zucchiatti: THE MONOCHROMATIC GAMMA BEAM FACILITY OF FRASCATI LEALE LABORATORY.

Servizio Documentazione
dei Laboratori Nazionali di Frascati
Cas. Postale 13 - Frascati (Roma)

Laboratori Nazionali di Frascati
Servizio Documentazione

LNF-77/45(R)
26 Agosto 1977

G. P. Capitani, E. De Sanctis, C. Guaraldo, G. Ricco(*), M. Sanzone(*), R. Scrimaglio and A. Zucchiatti(*): THE MONOCHROMATIC GAMMA BEAM FACILITY OF FRASCATI LEALE LABORATORY.

1. - INTRODUCTION.

One difficulty in the investigation of photonuclear reactions with real photon is the lack of suitable powerful gamma sources of variable energy. Positron annihilation in flight has been widely used in recent years to obtain quasi-monochromatic photon beams[1]. However, because of the necessary double conversion (electrons to positrons and positrons annihilation), high current electron accelerators are needed with this technique.

In this paper we describe the LEALE (Laboratorio Esperienze Acceleratore Lineare Elettroni) monochromatic gamma beam facility from the Frascati linac positron beam[2]. In Sect. 2 is described the positron acceleration in the Frascati 450 MeV linear accelerator. In Sect. 3 the main features of the positron beam at the end of the transport channel in the LEALE area are reported, together with all concerns the positron beam handling. In Sect. 4 the characteristics of the monochromatic gamma beam from annihilation of positrons on hydrogen are described in detail.

2. - POSITRON ACCELERATION IN THE FRASCATI LINAC.

The Frascati linear accelerator[3] is made up of twelve sections: four low guides capable of accelerating 420 mA of electron beam to 65 MeV, and eight high energy guides capable of accelerating, together with the low energy ones, 100 mA of electron beam to 375 MeV. RF power to the guides is supplied by six Thomson-Varian Klystrons type CFTH TH 2014 (25 MW output peak power, 40% efficiency, 2856 Mc/sec (S-band) each pulsed by a modulator as power supply (4 μsec pulse lenght, 200 pulses per second, 8×10^{-4} duty cycle, 63 MW peak power to Klystrons).

Positrons are generated in a conversion target by bremmstrahlung production and subsequent pair production from the high current-low energy electron beam produced by the first four Sections of the linac. The system for the positron production includes:

a) the target, made of copper, one radiation lenght thick, disk shaped, water cooled. A second target made of pure tungsten (97.5 % W, 2.5 % Ni), one radiation lenght thick, race-track shaped, water cooled, is also available: it gives a higher positron yield (a factor 2.3) but, due to lower conductivity of tungsten, can be used only at low frequency ($\leq$ 30 p.p.s.);

b) an adapting magnetic lens made up of a short solenoid, extending 6.2 cm far from the immersed target and run at 17 700 Gauss. The half cyclotron period for 10 MeV positrons (energy corresponding to the maximum of the efficiency in the electron-positron conversion) is 6.2 cm;

(*) INFN - Sezione di Genova.

c) the eight high energy sections. Each section is equipped with a full lenght (5 meters) of solenoid producing an uniform static axial magnetic field of 2400 Gauss. The problem of solenoid misaligmment with respect to the Sections was solved by mounting soft iron plates at the beginning and at the end of each section, concentric with it. The plates are centered on the linac axis. This affects the fringing field configuration which tends to become centered with respect to the beam. The transverse magnetic field component, due to the solenoid being tilted with reference to the section centerline, is compensated using two steering fields per section.

The positron beam produced by the machine is used for injection into the Frascati storage ring ADONE and for nuclear physics experiments in the LEALE Loboratory, after the annihilation on a hydrogen target to give a secondary monochromatic gamma ray beam.

A typical positron energy spectrum at the end of the linac is given in Fig. 1. The positron

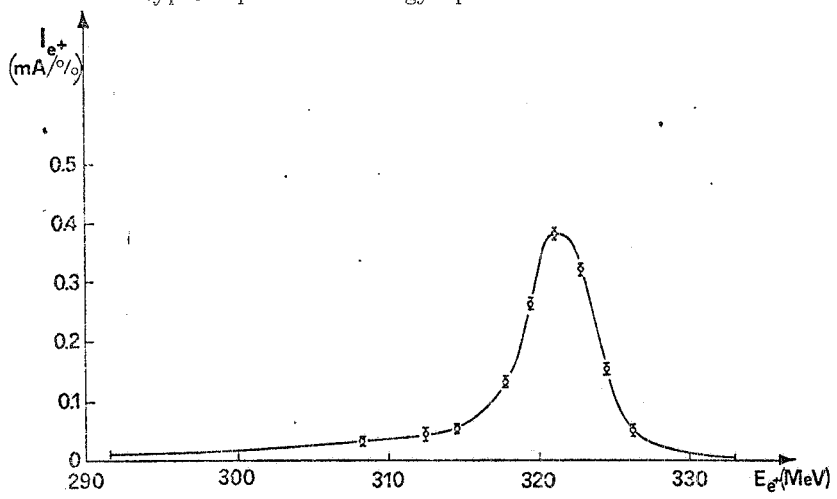

FIG. 1 - Peak positron current of the Frascati linac at 321 MeV within an acceptance of π x 10 mrad x mm. Electron beam on the converter: 250 mA at 80 MeV; pulse lenght 3.2 μsec; repetition rate: 50/16 p.p.s.; analysing slits: 1%. The total current integrated over the range 291÷333 MeV results in a peak of 930 μA. Positron current within 1% energy bin is 380 μA. (From ref(3)).

beam current was collected on a Faraday cup and measured with an integrator. In this case, electron beam peak current used for conversion was 250 mA at 80 MeV and the tungsten converter has been used. The total current obtained at the end of section 12, integrated over the the range 291÷333 MeV, but within an acceptance of πx10 mrad x mm, resulted in a peak of 930 μA. Positron current within 1% energy bin was 380 μA at 321 MeV.

3. - THE POSITRON BEAM.

3. 1. - The positron beam handling.

The positron beam trasport system has been already described in detail in ref. (4). The first part of the beam-handling, from the end of the linac up to the deviation system, is the same used to trasport the electron beam for the pion channel[5]. It consists (Fig. 2a) of three quadrupole doublets (Q_1-Q_2, Q_3-Q_4 and Q_5-Q_6) and four collimators (C_1÷C_4: 25-25-25 and 40 mm diameter, respectively).

The pulsed magnet inserted after the collimator C_1 allows the deflection of the beam in ADONE, or the transmission into the LEALE area, or the energy analysis of the beam itself. For this later operation, one beam pulse per second is deflected in an analysing magnet having as a detector in its focal plane a system of secondary emission monitors (hodoscope) which provides an on line measurement of the beam energy spectrum.

In order to gain in stability and to improve the transmission through the collimators, the strenghts K of the first two doublets of quadrupoles ($K = \sqrt{30\ e\ G/p}$, where G is the field gradient in KGauss/m and p the momentum in MeV/c) are such that $K_{Q1} = K_{Q3}$ and $K_{Q2} = K_{Q4}$. The doublet Q_5-Q_6 is necessary to maintain the beam dimensions quite constant. Fig. 2b shows the positron beam radial and vertical envelopes in the first part of the trasport channel.

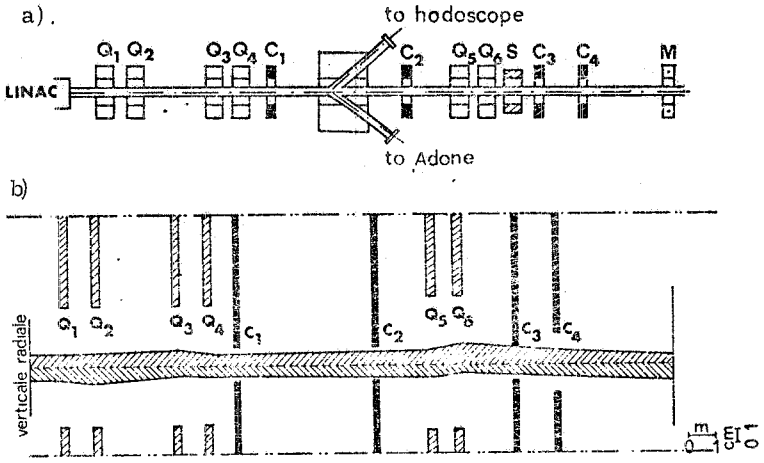

FIG. 2- a) The first part of the positron beam-handling. b) Positron beam radial and vertical envelopes in the first part of the transport channels. $Q_1 \div Q_6$ quadrupole magnets; $C_1 \div C_4$ collimators; S steering coils; M ferrite current monitor.

The second part of the beam handling is a conventional Penner type achromatic system, which gives a 45° It consists (Fig. 3a) of four deflecting magnets ($B_1 \div B_4$) with uniform field

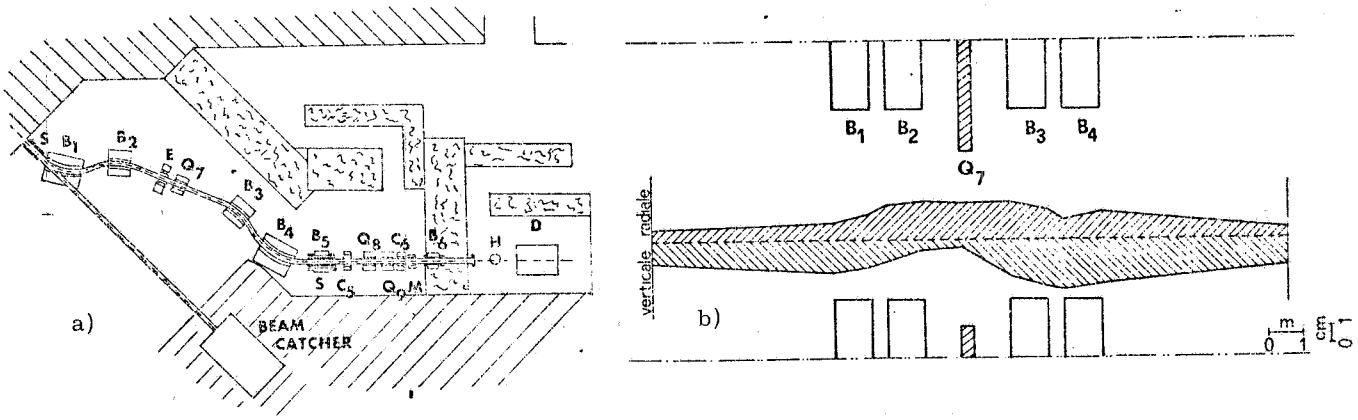

FIG. 3 - a) The second part of the positron beam-handling. b) Positron beam radial and vertical envelopes in the second part of the transport channel. $B_1 \div B_6$ bending magnets; $Q_7 \div Q_9$ quadrupole magnets; D damping magnet; S steering coils; E energy defining slits; M ferrite current monitor; $C_5 C_6$ collimators (7 and 6 mm diameter); H hydrogen annihilation target.

and non zero entrance and exit angles, in order to provide a double focusing. The deflection angles are, respectively, $\theta_{B_1} = \theta_{B_4} = 60^\circ$ and $\theta_{B_2} = \theta_{B_3} = 37.5^\circ$.

Two tantalum slits (E in Fig. 3a), 15 mm thick, in the symmetry plane of the achromatic system, allows the beam energy selection. The energy calibration of the slits have been performed by comparison with the positron energy spectrum measured by the hodoscope. Fig. 3b shows the positron beam radial and vertical envelopes in the second part of the transport channel.

Three pairs of steering coils along the line allow to centre the positron beam on the annihilation target. Size and position of the on the target are controlled observing with a TV camera the scintillation produced on a Ca W 0_4 screen. The beam spot has elliptical shape with 7 mm vertical semiaxial and 4 mm radial semiaxial.

A precise definition of the photon emission angle is obtained only through a very accurate alignment of the positron beam along the optical axis of the channel. It is possible to reach this goal by optimizing the transmission of the positron current through two removable copper collimators (C_5 and C_6, 7 mm and 6 mm diameter, respectively), before the annihilation target, by different

sets of steering coils. The final doublet of quadrupoles, Q_7 and Q_8, usually turned off, is just used to test the correct alignment, by verifying on the TV screen the absence of steering effects due to the quadrupole fields.

The positron incidence angle on the target may be changed between 0° and 1.5° by two bending magnets (B_5 and B_6 in Fig. 3a) which give a vertical deflection. As it is known[6](see Fig. 4), the increasing of the collection angle of the photon beam respect to the positron one, improves the annihilation to bremmstrahlung ratio. Meanwhile, intensity and energy resolution strongly decrease with angle.

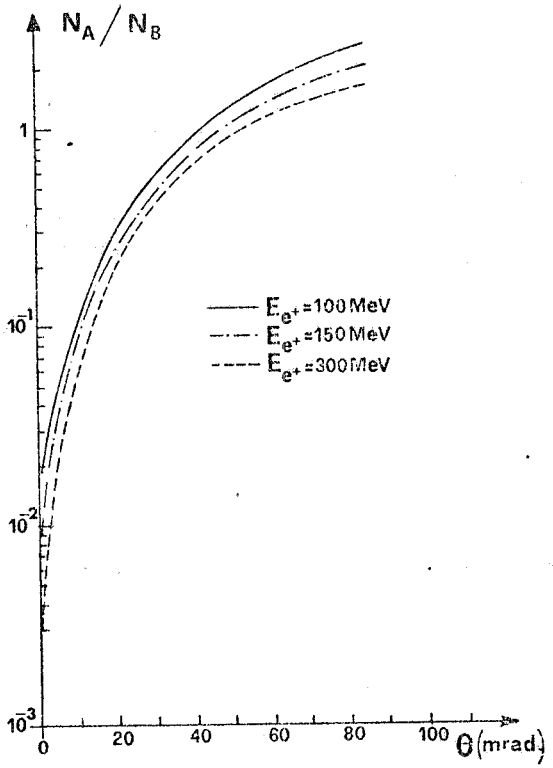

FIG. 4- Angular dependence of the annihilation/bremmstrahlung yields ratio N_A/N_B from a hydrogen target for three positron energy values.

3. 2. - The positron beam intensity.

The intensity of the positron beam is continuously monitored in three points of the transport channel (one of which is at the end of the line) with non intercepting current transformer, consisting in a ferrite toroid placed around the beam line[7]. The positron beam acts as the primary of the transformer, while the secondary is a 20 turns coil wrapped up on the toroid. The signal from the secondary feeds a low impedence preamplifier-integrator, placed near to the monitor. The preamplifier-integrator output signal is again amplified (H. P. amplifier mod. 462 A) and sent to the control room through about 60 m of coaxial cable (RG 213/U). With this set up the signal to noise ratio turns out to be about 10 : 1 for signals of some mV amplitude at the amplifier integrator output.

A calibration test pulse induced by a standard current is sent in a one loop coil wrapped up on the ferrite toroid some μs after the beam pulse, so that, by comparing on a scope the two signals (beam signal, test signal) is possible to have an immediate feeling of what happens during the beam turning. A block diagram of the whole system is shown in Fig. 5.

The ferrite toroid can be also used as an intensity monitor by operating in a different way described in the second of the ref. (7). The overall accuracy, strongly depending on how accurately is known the test pulse and on its similarity to the beam pulse, can be extimated of the order of some per cent.

The absolute value of the positron current on the target can be also measured by a Faraday cup (used also as beam catcher) put in the focal plane of a damping magnet after the annihilation target (Fig. 6). This magnet sweeps off from the photon beam the positrons which have not undergone

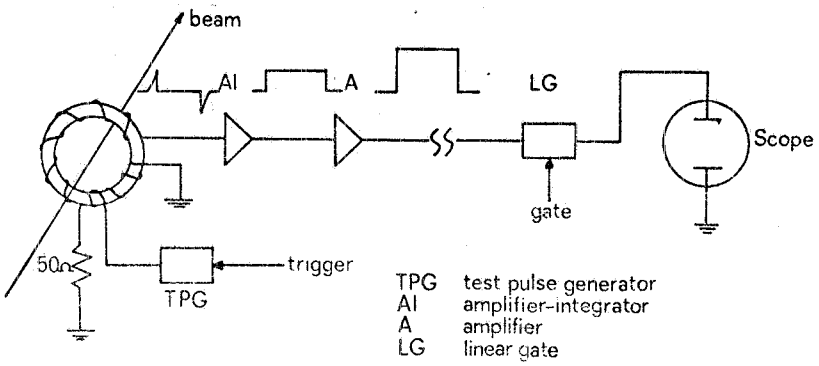

FIG. 5- Block diagram of the electronic layout of the ferrite toroid monitor.

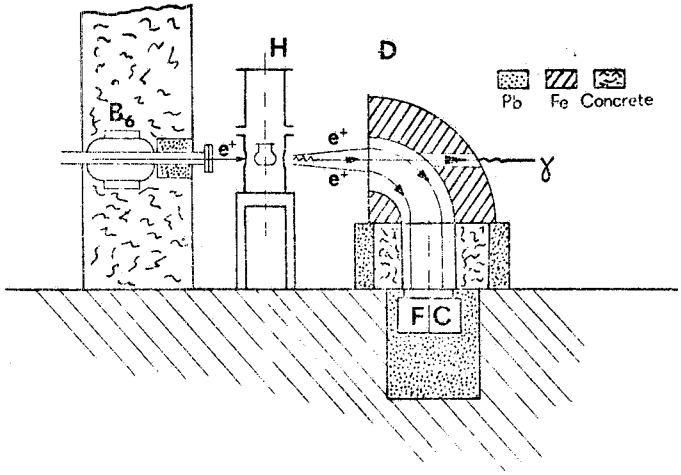

FIG. 6 - The positrons beam-catcher. B_6 bending magnet; D damping magnet; H hydrogen target; FC Faraday cup.

annihilation. The Faraday cup for positrons has a central core made up of cylindrical lead beam stopper, 30 cm diameter, total thickness 15 cm, which allows the absorption of up to 400 MeV positrons. The core is mounted inside a static vacuum envelope closed by a thin ($\approx$ 2 mm) entrance window.

The collected charge is picked up from the central core by means of a special triaxial connector provided with a ceramic insulator and a guard ring. The mean current is sent directly to a standard current integrator and digitizer (ORTEC Mod. 439). The vacuum container of the Faraday cup is connected to the general ground of the experimental area, while the guard shielding is connected, through the triaxial connector guard ring, to the integrator virtual ground.

In Fig. 7 is reported the peak positron current measured in the energy range 80÷300 MeV, with the tungsten converter (repetion rate 5 p. p. s.).

In Fig. 8 the positron yields versus energy, for those existing facilities used to produce photon beams by positron annihilation[1] are reported. As it is possible to see from the figure, the LEALE facility of Frascati features appear particularly interesting. The Frascati values have been evaluated for the copper converter and at a repetition rate of 200 p. p. s.

3. 3. - The positron energy spectrum.

The positron energy spectrum has been determind at various energies measuring the charge collected by the Faraday cup for different positions of the energy defining slits (E in Fig. 3a). As an example, Fig. 9 show the spectra measured at E_{e+}= 99 MeV and 200 MeV (solid lines). In the figure the spectra (hystograms) obtained with the hodoscope at the end of the linac are shown for comparison.

In Fig. 7 the energy resolution of the positron beam in the full energy range 80÷300 MeV is reported.

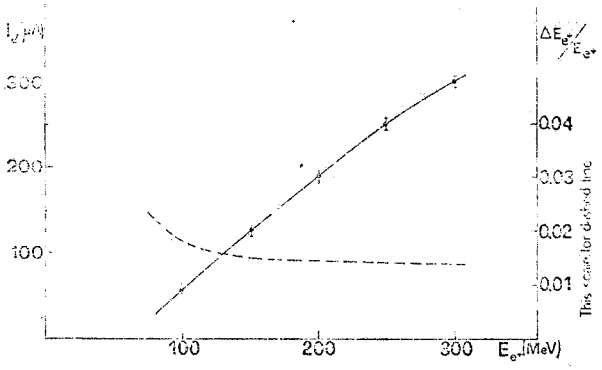

FIG. 7- Positron peak current on the hydrogen target (solid line) and FWHM energy resolution (dashed line) versus energy (tungsten converter, repetition rate 5 p. p. s.).

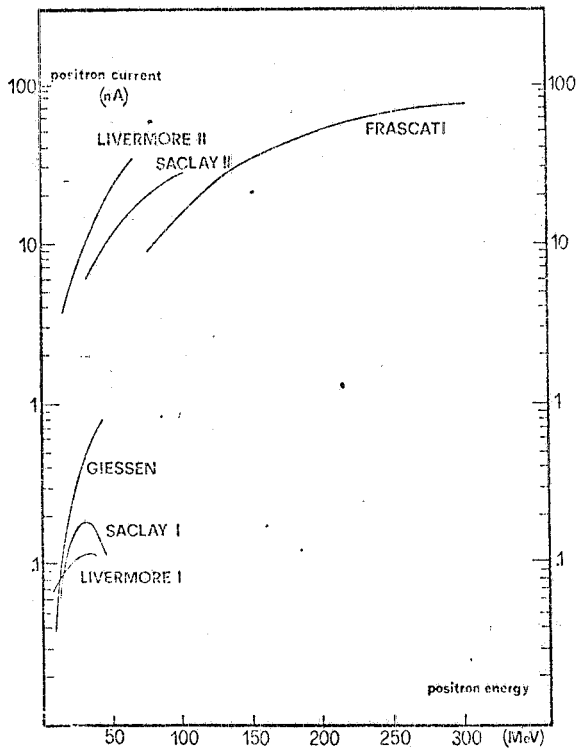

FIG. 8- Positron yields versus energy for the existing facilities used to produce photon beams by positron annihilation.

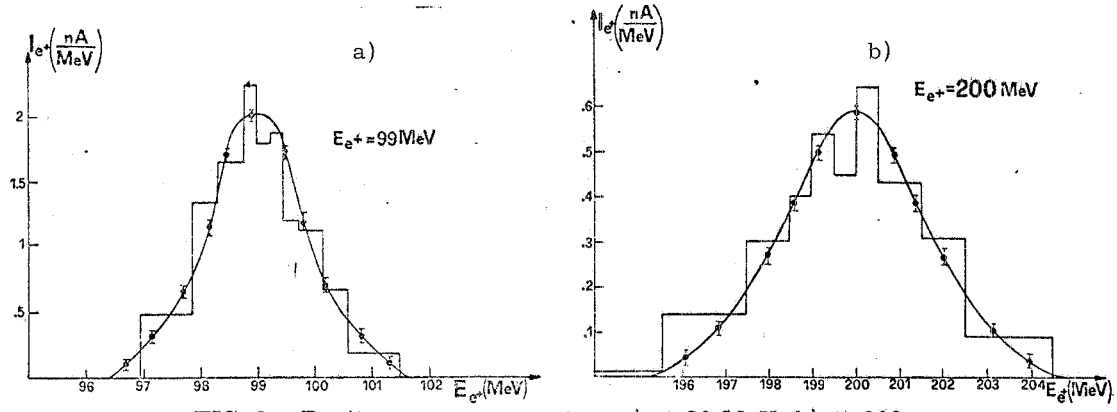

FIG. 9 - Positron energy spectra: a) at 99 MeV; b) at 200 MeV. The hystograms are obtained on the hodoscope at the end of the linac. The solid lines refer to the current measured by the Faraday cup for different positions of the energy defining slits (repetition rate 50 Hz , copper converter).

4. - THE PHOTON BEAM.

4. 1. - The photon beam line.

Positrons leave the vacuum pipe through a thin aluminum window, $6.7\ 10^{-4}$ radiation lenghts thick, annihilate in a cylindrical liquid hydrogen target, then are deflected down in the Faraday cup by the damping magnet D (Fig. 6).

The hydrogen cell is a capton cylinder, 105 mm long, 55 mm diameter (wall thickness 0.125 mm). The cell is contained in a vacuum steel tank presenting to the beam two thin capton windows,

0. 1 mm thick each. The cell can be rotated through 90°, in order to utilize two hydrogen thicknesses, 0. 011 or 0. 005 radiation lenghts, respectively.

Two collimators (C_7 and C_8 in Fig. 10) collect the photons emerging from the target. The first

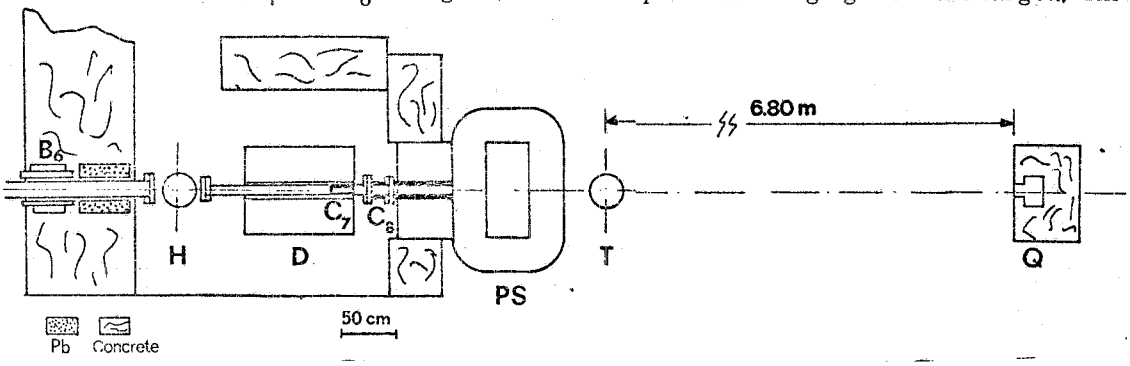

FIG. 10 - Photon beam layout. B_6 bending magnet; H hydrogen target; D damping magnet; PS pair spectrometer; T experimental target; C_7C_8 collimators; Q quantameter.

one, iron made up, 2 cm diameter, 11. 9 radiation lenghts thick, is inserted in the yoke of the damping magnet. The second one, lead made up, of variable diameter from 1. 5 cm up to 1. 9 cm, is 89 radiation lenghts thick.

A rectangular flat pole C-magnet (dimensions 10 x 90 cm^2, 15 cm gap, PS in Fig. 10) will be used as an on-line pairs spectrometer (momentum acceptance $\sim$ 14%; resolution better than 0.17%; energy dispersion $\sim$ 0. 77 MeV/cm; detectors: two proportional wire chambers 26 x 13 cm^2 useful areas) (see ref. (8)).

4. 2. - Theoretical calculation of the photon yield.

The theoretical calculation of the annihilation yield from a hydrogen target has been performed (see ref. (6)) by taking into account the positron beam characteristics, the multiple scattering and the energy loss in the target.

In Table I are summarized the main features of the results obtained from a 150 MeV po-

TABLE I - Main features of the annihilation photon yield from a 150 MeV positron beam on a hydrogen target.

Hydrogen target thickness (g. /cm^2)	Photon collection angle (mrad)	$\frac{N_\gamma}{N_{e^+}\Delta\Omega}$ (sterad^{-1})	$\Delta E_\gamma / E_\gamma$	R_γ
0. 7	0 ÷ 5. 8	2. 40	1. 5	3. 3 10^{-2}
	0 ÷ 8. 75	2. 25	1. 5	3. 8 10^{-2}
	0 ÷ 17. 5	1. 10	2	4. 0 10^{-2}
	0 ÷ 17. 5(*)	0. 21	2	6. 2 10^{-2}
	17. 5 ÷ 26	0. 21	6. 5	2. 4 10^{-1}
	17. 5 ÷ 35	0. 14	9	2. 7 10^{-1}
0. 35	0 ÷ 5. 8	1. 89	1	2. 8 10^{-2}
	0 ÷ 8. 75	1. 26	1	3. 3 10^{-2}
	0 ÷ 17. 5	0. 52	1	3. 9 10^{-2}
	17. 5 ÷ 26	0. 08	5	2. 6 10^{-1}
	17. 5 ÷ 35	0. 97	8	3. 0 10^{-1}

(*) with 200 g /cm^2 of HLi hardener

sitron beam. In column 1 the annihilation target thickness is reported, in column 2 the photon collection angle. In column 3 the total number of annihilation photons per incident positron, produced in the unitary solid angle, is reported. The column 4 gives the FWHM energy resolution $\Delta E_\gamma / E_\gamma$ of the annihilation peak. Finally, in column 5 is reported the ratio

$$R_\gamma = 2 \frac{N_\gamma (e^+) - N_\gamma (e^-)}{N_\gamma (e^+) + N_\gamma (e^-)} ,$$

where $N_\gamma (e^\pm)$ is the number of photons with energy $E_\gamma \geq 15$ MeV produced from the positron on the electron beam. The interest of the above ratio lies in the fact that it is possible to subtract the contribution of bremmstrahlung photons, making the difference of the reaction production yields from the collision on the same hydrogen target of e^+ and e^- beams with the same features.

In Fig. 11 the results of the calculation performed for a 0.011 radiation lenghts thick hydro-

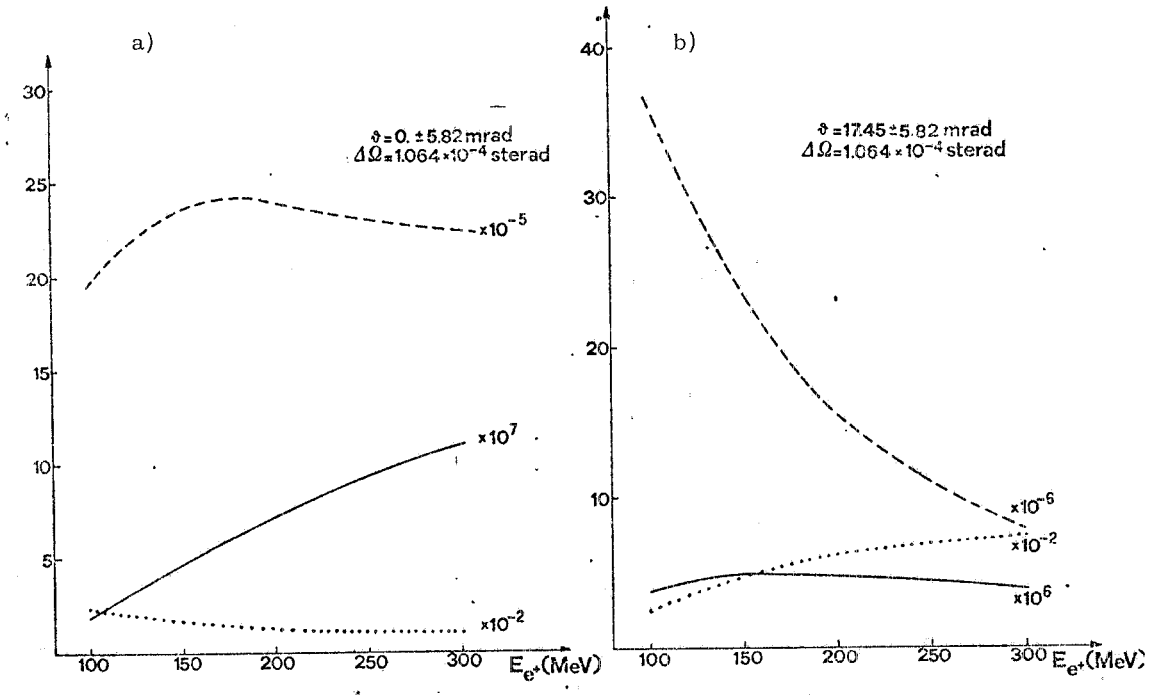

FIG. 11 - Photon beam features for 0.011 radiation lenghts hydrogen target at a) 0 ± 5.82 mrad and b) 17.5 ± 5.82 mrad photon collection angle. The dashed lines give the number of photons per incident positron. The solid lines give the number of annihilation photons per second. The dotted lines give the FWHM annihilation peak resolution.

gen target; at two different angular collection conditions, in the energy range 100÷300 MeV, are given. The dashed curves give the number of annihilation photons per incident positron. The solid line give the number of annihilation photons per second (it is the product of the dashed curve for the measured positron intensity of Fig. 7. The dotted curves give the FWHM energy resolution of the annihilation peak.

4. 3. - Photon beam features measurements.

Photon yield measurements are performed with the aid of a Wilson type quantameter modified in the integration system according to Komar suggestions[9] to obtain a constant sensitivity in

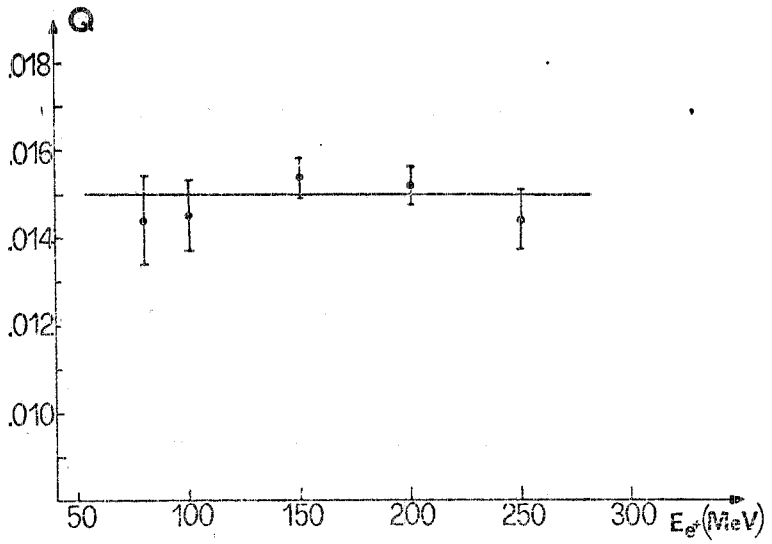

FIG. 12- Photon quantameter response.

the energy range 5 MeV÷ 5 GeV. In Fig. 12 are reported the values of the number of equivalent quanta per incident positron, $Q = R/(S\,E_{e+})$, measured at several positron energies. R and S are respectively the response and the sensitivity of the quantameter and E_{e+} is the positron energy. These measurements have been performed using a copper positron-photon converter 0. 015 radiation lenghts thick and without any collimation for the photon beam. The errors are mainly due to incertainties in the values of the quantameter sensitivity as deduced from ref. (9). In Fig. 12 the solid line refer to the calculated value of Q. The agreement between the experimental points and the calculation makes us confident on the reliability of the quantameter response.

Some measurements of the quantity Q at the energies 80 MeV, 150 MeV, 200 MeV have been performed also using a NBS P2 standard ionization chamber. The obtained values are in a fairly good agreement with those measured with the quantameter.

Preliminary measurements of photon energy spectrum have been performed using a small flat pole magnet (sizes 20 x 30 cm^2 and gap 1. 5 cm high) as pairs spectrometer[10] (details of the measurements are given elsewhere[2,11]). The small gap and the optical properties of the magnet have limited the photon collection angle to about 8×10^{-6} sterad.

The photon spectra obtained at the positron energy of 200 MeV are reported in Figg. 13 and 14 . In Fig. 13 are reported the data collected in two measurements done at $\theta = 17.5 \pm 0.5$ mrad using converters of two different thicknesses (0. 4 mm and 0. 8 mm). The measurement at $\theta = 0.0 \pm 0.5$ mrad (Fig. 14) has been performed with a 0. 06 mm thick converter, in order to reduce the multiple scattering effects.

Both the spectra show a peak at the correct annihilation energy, with a bremmstrahlung continuous tail. The annihilation bremmstrahlung ratio as well as the peak resolution are very sensitive to the collection angle, as expected. In this respect, during the measurements care has been taken to keep stable the ratio between positron and photon intensities.

Different background sources have been accurately investigated: annihilation target off background and random coincidences between positron and electron arms. In Figg. 13 and 14 the total background has been subtracted: the large experimental errors are due to poor statistics, because the strong collimation required by the spectrometer gap, cut down drastically the photon beam intensity.

In order to extract the annihilation peak from the total photon spectrum we have performed measurements using hydrogen and copper annihilation targets, 0. 011 radiation lenghts thick each. The photon spectra from the copper target show a typical bremmstrahlung energy dependence with a small amount of annihilation on the head. The hydrogen minus copper difference spectra, correspond therefore to the contribution, only slightly underestimated, of the annihilation photon in hydrogen.

The annihilation photon spectrum from hydrogen can be evaluated starting from the electromagnetic cross section and taking into account all the target thickness effects[6]. The theoretical spectrum corresponding to the geometrical set up of our experiment has been folded with a Gaussian resolution function one of $\sim$ 9 MeV FWHM to take into account the finite spectometer resolution, the

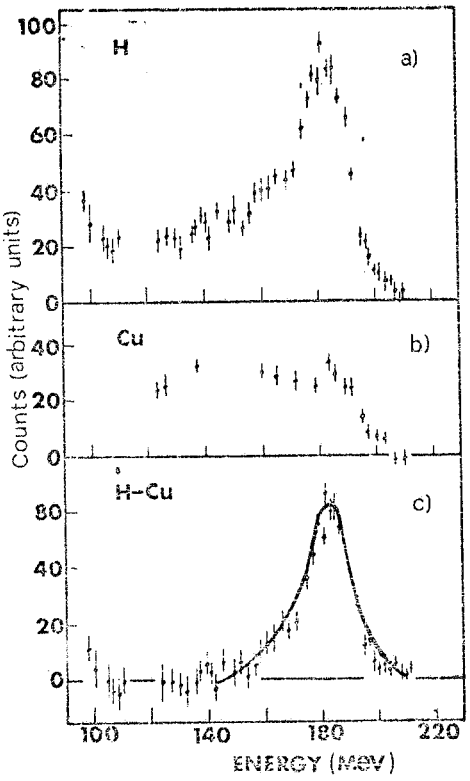

FIG. 13- Photon energy spectra at $\theta = 17.5 \pm 0.5$ mrad.

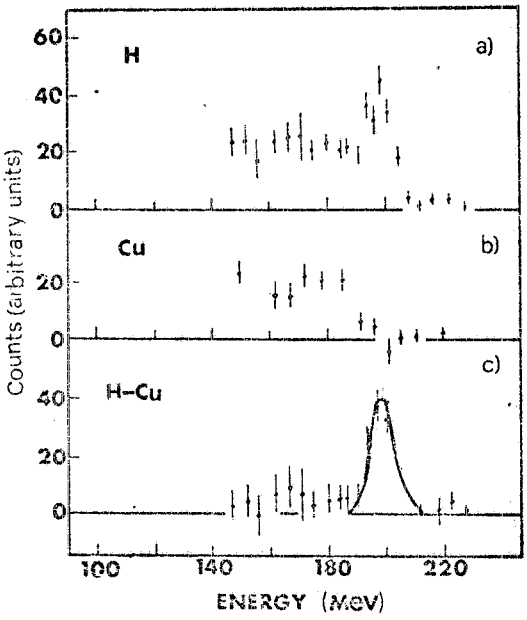

FIG. 14 - Photon spectra at $\theta = 0 \pm 0.5$ mrad.

other one, of $\sim$ 3 MeV FWHM to take into account the positron beam energy resolution. The final result, plotted as a continuous curve in Figg. 13 and 14, shows a fairly good agreement between theory and experiment for what concerns the absolute values ($N_\gamma / N_{e^+} = 2. 10^{-5}$ at 0 mrad, and $= 2. 10^{-4}$ at 17. 5 mrad) and the annihilation peak intrinsic resolutions (FWHM = 1% at 0 mrad, and = 4. 5% at 17. 5 mrad). Therefore we can be confident an our calculation of the photon beam features that we have summarized in Fig. 11 in two conditions suitable for photoreaction experiments.

The authors wish to thank Prof. R. Malvano for several very usefull discussions and Mrs. M. Albicocco, E. Durante, S. Faini, A. Macioce, C. Marchetti, V. Pucci, S. Romani, A. Rottura, D. Santoni and A. Viticchie for their continuous technical assistance and the Frascati linac staff for efficiency in running the machine.

REFERENCES

1) J. Miller, C. Schuhl, G. Tamas and C. Tzara, Jour. Phys. Radium, 21, 296 (1960); Nuclear Phys., 32,236 (1962) (Laboratory of SaclayI).
- E. G. Fuller, Proc. Int. Conf. on Phonuclear Reactions and Applications (Asilomar, 1973) pag. 1201 (Laboratories of NBS, Livermore II, Mainz).
- U. Kneissl, E. A. Koop, G. Kuhl, K. H. Leister and A. Weller, Nuclear and Meth., 127, 1 (1975) (Laboratory of Giessen).
- C. P. Jupiter, N. E. Hansen, R. E. Shafer and S. C. Fults; Nuclear Inst. and Meth., 121, 866 (1961) (Laboratory of Livermore I).
- C. G. Schuhl, Proc. Int. Conf. on Few Body Problems in Nuclear and Particle Physiscs (Quebec, 1974), p. 788; Proc. Int. Conf. on Photonuclear Reactions and Applications (Asilomar, 1973), p. 1249; R. Bergere: private communication (Laboratory of Saclay II).
- D. Blum, J. Boucrot, B. Grossetête, W. Mc Gill and H. Nguyen Ngoc: Nuclear Instr. and Meth., 115, 553 (1974) (Laboratory of Orsay).
2) G. P. Capitani, E. De Sanctis, C. Guaraldo, G. Ricco, M. Sanzone, R. Scrimaglio and A. Zucchiatti (Proc. Int. Conf. on Electro- and Photonuclear Reactions Erice 1976) Lecture Notes in Physics 62, pag. 199.
3) Varian Associates Technical Report R 63, April 24 (1963).
- F. Amman and R. Andreani: Frascati Report LNF-63/46 (1963).
- C. Nunan, IEEE Trans. on Nuclear Sci. NS-12, 465 (1965).
- F. Amman, R. Andreani, J. Haimson and C. Nunan: Frascati Report LNF-66/69 (1966).
4) G. P. Capitani, E. De Sanctis, S. Faini, C. Guaraldo, R. Malvano, G. Ricco, M. Sanzone and R. Scrimaglio: Frascati Report LNF- 72/99 (1972).
5) R. Barbini, S. Faini, C. Guaraldo, C. Schaerf and R. Scrimaglio, Nuclear Instr. and Meth. 115, 85 (1974).
6) E. Mancini and M. Sanzone, Nuclear Instr. and Meth. 66, 87 (1968).
7) S. N. Gardiner, J. L. Matthews and R. O. Owens, Nuclear Instr. and Meth., 87,285 (1970).
- M. Albicocco, G. P. Capitani, Frascati report (in press).
- G. Renzler, Frascati report , LNF-65/37 (1965).
8) G. P. Capitani et al., Frascati report (in press).
9) A. O. Komar, S. P. Kruglov and I. V. Lopator, Nuclear Instr. and Meth., 82, 125 (1970).
10) P. Banvenuto, D. Fabbri, E. Lodi Rizzini, L. Maiani, M. Napolitano, A. Piazza, V. Rossi, G. Susinno and L. Votano, Frascati report LNF-71/76 (1971).
11) G. P. Capitani, E. De Sanctis, S. Faini, C. Guaraldo, G. Ricco, M. Sanzone, R. Scrimaglio and A. Zucchiatti, Frascati report LNF-76/27 (1976).
- G. P. Capitani, E. De Sanctis, S. Faini, C. Guaraldo, R. Scrimaglio, G. Ricco, M. Sanzone and A. Zucchiatti, Lett. Nuovo Cimento, 16, 453 (1976).